Comparison of Sparse Image Descriptors for Eyes Detection in Thermal Images

Mateusz Knapik and Bogusław Cyganek
Department of Electronics, AGH University of Science and Technology, Kraków, Poland

Keywords: Eye Detection, Sparse Descriptors, Surf Descriptor, Daisy Descriptor, Thermal Imaging, Operator Monitoring.

Abstract: Eye detection and localization are basic steps in many computer systems aimed at human fatigue monitoring. In this paper we evaluate performance of two sparse image descriptors for eye detection in the long-range IR spectrum. In the training phase, sparse descriptors of the training images are computed and used to create features vocabulary. Final detections are done using bag-of-words approach and additional heuristic for geometric constraints. Several thermal video sequences were recorded to allow for quantitive analysis of this approach. Experimental results show that our method achieves high accuracy in real conditions.

1 INTRODUCTION

Behavior and alertness level of an operator play essential role in both people's safety as well as in avoiding economic losses. Real-time monitoring of individuals operating machinery and various vehicles is a subject of constant innovation in recent years. Such systems must cope with wide range of difficult conditions like noise, temperature, day and night illumination (Cyganek, 2007). They must be also able to provide correct response in presence of variability in appearance and behavior of human subjects.

For camera-based solutions, thermal long range IR imaging is gaining attraction in recent years, spurring both industrial solutions and research projects (Ji and Yang, 2002; Saradadevi and Bajaj, 2008; Azim et al., 2009; Fan et al., 2009; Cyganek and Gruszczyński, 2014; Shah et al., 2014; Wang et al., 2013; Strąkowska and Strąkowski, 2015; Marzec et al., 2016; Ribeiro et al., 2017). Unlike visible light sensors, long range IR cameras can operate with no external lighting even in total darkness. On the other hand, they are insensitive to even extreme visible lighting conditions frequently encountered in car conditions. Other challenging factors for visible light cameras, like, for example, skin color or camouflage makeup, are eliminated with thermal imaging. This properties makes them a viable alternative for classic cameras. Also, a supporting factor is growing availability of low-cost long-infrared spectrum sensors.

However, proper image processing and analysis methods are needed to create end-to-end solution. A system for tiredness level monitoring, which is based on facial features recognition, is composed of many smaller subsystems such as data acquisition, image processing and analysis for behavioral modeling. Almost always, one of the task involved in detection of the facial landmarks is the eye detection step. This paper evaluates performance of two sparse image descriptors when used for human eyes detection and localization in thermal images. The data processing path is composed of computation of either the Speeded Up Robust Features (SURF) (Bay et al., 2008) or DAISY (Tola et al., 2010) descriptors on a dense grid. Then clustering to achieve distinctive prototype patterns is applied. Further on there are modules for matching to vocabulary, similarity distance computation and finally geometric constraints verification. Contrary to other techniques, visibility of both eyes in an image is not required. The proposed method can be used in many domains, ranging from surveillance, entertainment or medical imaging.

Rest of this paper is organized as follows: Section 2 describes the existing state-of-the-art works that are related to the proposed system. Section 3 is an overview of the system architecture and theory behind methods used throughout this paper. Section 4 presents the results of conducted experiments to ascertain scientific validity of presented system. Finally, Section 5 presents our conclusions.

Knapik, M. and Cyganek, B.
Comparison of Sparse Image Descriptors for Eyes Detection in Thermal Images.
DOI: 10.5220/0007576506380644
In *Proceedings of the 14th International Joint Conference on Computer Vision, Imaging and Computer Graphics Theory and Applications (VISIGRAPP 2019)*, pages 638-644
ISBN: 978-989-758-354-4

2 RELATED WORKS

In this section general overview of the state-of-the-art works related to localization of facial areas in infrared spectrum is presented and discussed.

For near range infrared (NIR) spectra, system for eye detection was proposed by Cyganek and Gruszczyński (Cyganek and Gruszczyński, 2014). In order to detect and localize eyes, NIR images are fed into cascade of classifiers. Specialized iris-pupil model is used to determine initial regions of interest. Tensor classifier is then used to select the most probable pair of ROIs. Authors reported accuracy of over 96%.

For thermal imaging, currently existing works are mostly suited for a constrained imaging conditions, i.e. both eyes have to be present in the frame for algorithm to work correctly.

Wang et al. (Wang et al., 2013) proposed system for automatic eyes localization. Haar-like features boosted with Adaboost algorithm are used for determining 15 subregions of face area, determining the eyes position. Additionally, for situations when subject wears glasses, their system first tries to localize centers of each lens. However, face region is obtained by binarization and pixel summation, so presence of any objects with temperature similar to the human subject can affect the process and decrease its performance.

Face tracking method in long-range IR based systems was proposed by Strąkowska et al. (Strąkowska and Strąkowski, 2015). It is based on a principle, that corners of the human eyes are the hottest regions of the face. In their approach, face area is localized using modified binarization algorithm. Then H-maxima transformation is used to preprocess the image and select regions of interests. Final result is based on calculation of geometrical distances between proposed regions.

In 2016, Marzec et al. in (Marzec et al., 2016) presented new approach for fast eyes localization in thermal images. Two-stage system consists of face area detector and classifier based on multilayer perceptron neural network. Authors claims high accuracy of their method, however similar constraints as in Wang's methods are present, for example, both eyes have to be visible to obtain regions of interest for further processing.

On the other hand, face detection in thermal imaging using template matching was recently presented by Ribeiro et al. (Ribeiro et al., 2017). Their proposed method achieves good accuracy and low computational complexity. Authors also report that the method based on the Haar cascades, often used for visible light spectrum, can yield better results, but training process of such classifier requires large amount of data and can be time consuming.

For features detection, Lowe presented algorithm called Scale-invariant Feature Transform (SIFT) (Lowe, 2004). It is one of the most well-known algorithms for detection and descriptor generation of local features in images. Due to it's high invariance to uniform scaling, orientation and illumination changes it is used in many applications including image-stitching, video tracking and object detection, to name a few.

Bay et al. proposed scale- and rotation-invariant feature descriptor and complementary keypoint detector called Speeded Up Robust Features (SURF) (Bay et al., 2008) as much faster alternative to SIFT. For detection of points of interest SURF uses an approximation of the determinant of the Hessian blob detector. Authors claims that SURF is more robust than SIFT against different image transformations while being several times faster to compute at the same time.

Tola et al. introduced feature descriptor called DAISY (Tola et al., 2010), designed specifically to be efficient when computed densely, i.e. for 3D reconstruction from the wide-baseline image pairs. It requires less computational power than SIFT. In comparison to SURF, it is claimed not to introduce artifacts that degrade matching performance when computed on a dense grid.

Bag-of-words image categorization methods were presented in a past by several researchers (Csurka et al., 2004; Lazebnik et al., 2006; Fulkerson et al., 2008) colorredboth for image classification as well as feature detection. Only recently BoW method was also applied for feature detection in other spectra (Malpani et al., 2016). In their work, Malpani et al. presented system for human detection and localization in thermal images.

To the best of our knowledge, the presented paper is a first comparison of SURF and DAISY descriptors for eye detection in thermal images.

3 EYE LOCALIZATION IN THERMAL IMAGES

An architecture of the eye detection module described in this paper is presented in Fig. 1. Further sections present detailed description of each of the visible modules. In our method, SURF and DAISY feature descriptors are used for feature extraction. Either feature description technique was used separately on the same set of images and the results have been compared. Facial-features localization is later done using sparse representation of a thermal image. Training

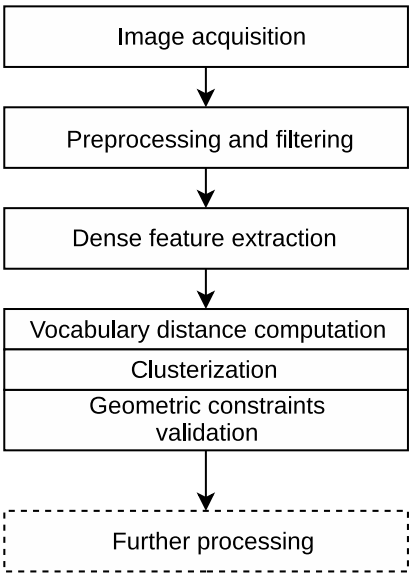

Figure 1: Eye detection system architecture.

images of eyes are used to create vocabulary of descriptors in a training phase. Later, descriptors extracted from new images are compared to the dictionary to compute the similarity measure. Statistical modelling of a training data is used to remove features that are dissimilar from the trained patterns. High confidence features are gathered into clusters and final eye candidates are chosen using series of geometrical checks.

3.1 Contrast Enhancement

One of the main characteristics of thermal images is their low contrast. Low variance in temperature between facial landmarks can decrease the performance of feature detection modules. In our method, stream of the thermal images from the acquisition module are preprocessed using multi-scale local contrast enhancement method proposed by Cvetkovic et al. (Cvetkovic et al., 2009).

Every pixel of the input image is processed with local-spatial filter computed as follows:

$$o_i = i_i + (i_i - m(i_i)) \tag{1}$$

where i_i is the input pixel intensity and m is the mean value around the pixel i_i in a window of size 3×3 pixels calculated using Equation (2). Size of the window has been chosen empirically to suite the low resolution of the input images.

$$m(i_i(x,y)) = \frac{1}{9} \sum_{s=-1}^{1} \sum_{p=-1}^{1} i_i(x+s, y+p) \tag{2}$$

Images before and after contrast enhancement can be seen in Fig. 2.

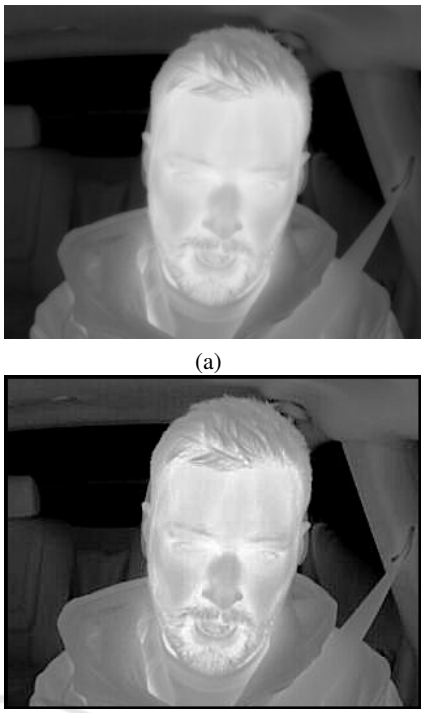

(a)

(b)

Figure 2: Thermal image before (upper) and after contrast enhancement (lower).

3.2 Vocabulary Extraction

Bag-of-words dictionary is created in the training phase that starts with a computation of a dense grid of feature descriptors on the training images of eyes taken in long-range infrared spectrum. Dimensions of the grid have been selected empirically and set to d_{desc}. Feature descriptors obtained in such way could be used directly to form a feature vocabulary, however to increase the generalization of our model feature reduction technique called *k-means* clustering have been applied. This iterative process groups together similar descriptors to form k visual words from the clusters centroids. Because the size of the dictionary impacts the detection effectiveness, it was chosen empirically, as will be shown later.

To measure the distance of a single feature from the dictionary, an Euclidian metric is used. It is calculated as follows:

$$d(f,v) = min \left[\sqrt{(f_0 - x_0^0)^2 + \cdots + (f_{n-1} - x_{n-1}^0)^2}, \cdots, \sqrt{(f_0 - x_0^{k-1})^2 + \cdots + (f_{n-1} - x_{n-1}^{k-1})^2} \right] \tag{3}$$

Table 1: Parameters used in the presented algorithms.

Parameter	Value	Used in	Comment
d_{desc}	1 to 3 pixels	Dense grid sampling	Distance in vertical and horizontal direction between feature descriptors
w_h, w_w	2 by 2	Distance comparison	How many neighboring features distances are used for comparison
v_{size}	100 to 200 words	Distance comparison	Number of visual words in the dictionary
d_c	10 or 15 pixels	Algorithm 1	Maximal distance in pixels between neighboring points
g_{ecc}	0.85	Algorithm 2	Eccentricity limit for cluster
g_{min}, g_{max}	2x2 pixels, 50x50 pixels	Algorithm 2	Cluster length and width constraints
e_{min}, e_{max}	0.8, 3	Algorithm 2	Distance ratio between two eyes
θ_{max}	60 deg	Algorithm 2	Maximal angle between two clusters

where f is new feature, $x_0^i, x_1^i, \cdots, x_{k-1}^i$ are the elements of ith visual word from the vocabulary, n denotes the size of a single word and k denotes the size of the whole vocabulary.

3.3 Distance Thresholding

Because human eyes will occupy relatively small area of the whole image and the fact, that feature descriptors are computed on a dense grid, our system employs features reduction method based on a statistical modelling. To reduce number of potential regions of interest, we compare the distance $d(f,v)$ to a threshold value obtained in a training phase. A mean plus two standard deviations method described in (Miller, 1991) has been used in experiments presented in this paper and was computed as follows

$$t_\sigma = \overline{D} + 2 \cdot \sqrt{\frac{1}{N}\sum_{i=1}^{N}\left(d(f_i,v) - \overline{D}\right)^2} \qquad (4)$$

where N is the number of features in a training set, $d(f_i,v)$ is the distance of an ith training feature (before clustering) from the vocabulary v and $\overline{D}$ is an average distance of all training features from vocabulary v.

In detection phase, feature or group of features will not be passed to further processing blocks if it's distance from vocabulary is bigger than the t_σ threshold. To improve robustness, in our experiments we used sum of distances of $w_h \times w_w$ features, both to compute threshold as well as in detection phase.

Visualization of thresholding process can be seen in Fig. 3(b).

3.4 Detection

Detection and localization tasks can be started after the training phase is done. For every new image dense grid of feature descriptors with the same grid dimensions as in a training phase is computed and distance 3 is calculated for every feature. This creates a map of distances between local descriptors and trained vocabulary. A sliding window of size $w_x \times w_y$ is then used to compute average distance of neighboring features. This is compared to the t_σ threshold and inliers are put into a priority queue of length L_f, which is ordered by the distance value. The lower the value, the higher the position in the queue.

To further decrease the amount of features, clustering method called Salient Point Clustering (SPC) is employed and every cluster is additionally approximated by an ellipse using central moments technique. Both of these were presented and described in (Cyganek, 2013).

Algorithm 1 shows the implementation details of the SPC method using following definition of close neighboring points: two points a and b are considered as close neighbors if following inequality holds:

$$N\Big(a,b\Big) \leq d_c \qquad (5)$$

where N denotes the Euclidean distance and d_c stands for an arbitrary chosen threshold.

A center point of a cluster c is computed using the weighted average of every point, using it's distance value as a weight, using the following formulas.

$$d_{max} = \max\Big[D_c\Big] \qquad (6)$$

$$w_i = w_{max} - d_i \qquad (7)$$

$$W = \sum_i^N w_i \qquad (8)$$

$$p_c = \left(\frac{1}{W}\sum_i^N x_i \cdot w_i, \frac{1}{W}\sum_i^N y_i \cdot w_i\right) \qquad (9)$$

where D_c denotes set of distances of features in a cluster c, d_i is a distance of ith feature in a cluster, w_i is a weight for ith feature, W is the sum of weights, N is a number of features in a cluster c, x_i and y_i denote the position of an ith feature of cluster c in a dense features grid, and finally p_c is the center point of a cluster c.

Then the inertia tensor can be computed in terms of the central moments, as follows.

$$c_{ab} = \sum_{i=1}^{N}\sum_{j=1}^{N}(x_i - p_c^x)^a(y_i - p_c^y)^b \tag{10}$$

$$T = \begin{bmatrix} c_{20} & -c_{11} \\ -c_{11} & c_{02} \end{bmatrix} \tag{11}$$

To obtain length l_c and width w_c of the cluster c, following formulas are computed:

$$l_c = \sqrt{\lambda_1}, w_c = \sqrt{\lambda_2}, \lambda_1 \geq \lambda_2 \tag{12}$$

where λ_1 and λ_2 are eigenvalues of the inertia tensor T.

Clusters are then inserted into another priority queue of length L_c that is ordered by ascending value of the median of cluster's weights w_i.

Algorithm 1: Salient Point Clustering.

Input: Set of points p_{in}. Distance threshold d_c.
Output: Clusters of points

while p_{in} has elements **do**
  pop last element from p_{in} as s
  for all clusters c **do**
    c_0 is a first point in cluster c
    if inequality (5) holds for s and c_0 **then**
      add s to cluster c
      break
  if s is still not clustered **then**
    create new cluster, add s as a first point

As a last step, simple geometric constraints checks are made. Clusters must form ellipses of eccentricity lower than g_{ecc} and their length and width must be within chosen limits. Finally, if more than two clusters pass this criteria, their relative position, both the distance and the angle, is checked. These form the proposed eye regions. Detailed description of this process is shown in Algorithm 2.

Algorithm 2: Geometric verification.

Input: Clusters of points. Constants g_{ecc}, g_{min}, g_{max}, e_{min}, e_{max}, θ_{max}.
Output: Proposed eye regions

for every cluster c **do**
  if c eccentricity $\geq g_{ecc}$ **then**
    continue
  if c width $\geq g_{max}$ **or** length $\geq g_{max}$ **then**
    continue
  if c width $\leq g_{min}$ **or** length $\leq g_{min}$ **then**
    continue
  add c to *correct clusters* list
if *correct clusters* length == 0 **then**
  return empty list
else if *correct clusters* length == 1 **then**
  return one proposed eye region
else
  get first two clusters from correct clusters list as c_a and c_b
  set p_a, p_b to respective clusters centroids
  if $atan2(p_a, p_b) > \theta_{max}$ deg **then**
    return empty list
  D denotes the Euclidian distance between points
  if $D(p_a, p_b) < e_{min}$ or $D(p_a, p_b) > e_{max}$ **then**
    return empty list

4 EXPERIMENTAL RESULTS

The methods proposed in this article were implemented using Python language and well-known and publicly available libraries like numpy, scipy, scikit-learn and OpenCV. Experiments presented in this section were run on a laptop computer equipped with 16GB of RAM, and 4-core processor i7-6700HQ with the 2.6GHz clock. The 64-bit Windows® 10 operating system was used. Future implementations aimed at speedup are also possible, e.g. by utilizing parallel computing platforms, like CUDA® or OpenCL®.

Quantitive evaluation was done using our own thermal database that consist of over 3500 images of human faces from three participants with manually labeled ground-truth frames. Database was created using the FLIR® A35 camera that produces images of resolution 320×256 pixels. For the purpose of our comparison, number of experiments were conducted. The following research questions were stated:

- What is the accuracy of the proposed method?
- Is there a measurable benefit of using feature descriptor designed for dense sampling?

Average results of three repetitions of every experiment are presented. Before every test round dataset was randomly split in half to create training and validation subsets. Result from every frame was categorized in terms of true-positive (TP), true-negative (TN), false-positive (FP), and false-negative (FN) parameters and then F value was computed. Each correctly recognized eye position, that is, the difference between region found by an algorithm and the ground

Table 2: Results of detection accuracy experiments.

		F-value result											
		DAISY						SURF					
Vocabulary		100		150		200		100		150		200	
Cluster size		10	15	10	15	10	15	10	15	10	15	10	15
Step size	1	**0.808**	0.817	**0.802**	0.795	**0.785**	0.796	0.784	0.801	0.790	0.791	0.776	0.788
	2	0.755	**0.931**	0.747	**0.942**	0.747	**0.943**	0.688	0.846	0.671	0.827	0.677	0.861
	3	0.789	0.912	0.786	0.908	0.772	0.908	0.727	0.844	0.735	0.857	0.733	0.858

truth is less than 10 pixels (around 3% given the size of an input image), is reported as a true-positive. Every incorrectly detected eye is counted as false-positive. False-negative is increased when algorithm fails to detect an eye. Eyes not present in the picture and not reported by algorithm are counted as true-negative. Summary of the parameters used in the conducted experiments is presented in Table 1. Full results of the experiments are presented in Table 2.

To find optimal parameters for each type of feature descriptor many combinations of parameters were tested. Three different grid spacing were considered, from 1 to 3 pixels, alongside three different dictionary sizes, from 100 to 200 visual words and two sizes of clustering thresholds, 10 and 15 pixels. Bigger clusters in case of both descriptors increased the performance significantly. More features allowed to refine clusters size and find center point more accurately. However, it should be noted that clustering threshold is correlated with grid spacing. Very dense grid results in small intra-class difference between words. Increase in spatial distance between features allows for better utilization of vocabulary, therefore bigger clusters can be localized with better precision. This results in better detector performance. On the other hand, increasing vocabulary size had little effect on the efficacy of detection, even decreasing F-value in some cases. Low resolution and noise in the input images decrease the intra-class difference between computed descriptors, therefore expanding dictionary size does not bring radical performance increase while being computationally expensive. We checked the lowest and highest F-value for both descriptor types. Even in worst case scenario, the F-value is higher than 0.67 for SURF descriptor and 0.74 for DAISY descriptor which is quite good considering the vagueness of eye contours in thermal images. DAISY descriptor achieves around 6% better results on average, reaching over 0.94 F-value with fine-tuned grid and vocabulary size (0.86 for SURF). This results answer our second research question. In our experimental setup, a dictionary with 200 words, combined with cluster size of 15 pixels and grid step of 2 pixels, gave the overall best results for both types of descriptors.

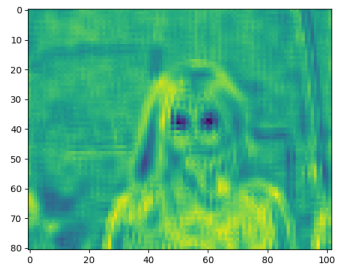

(a)

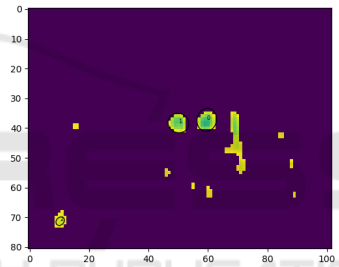

(b)

(c)

Figure 3: Distance map (top), corresponding map after thresholding and clustering (middle) and final detection result (bottom).

5 CONCLUSION

In this paper two types of local features descriptors are compared for usage in eye detection in thermal images system. Dense grid of feature descriptors is used to create a dictionary of visual words, that are

then used for eye regions detection and localization. As shown, the proposed system achieves high accuracy as well as proves the benefits of using feature descriptor designed with dense sampling in mind. There is also room for improvements in implementation after which it can operate in real-time. The proposed system can be also used in other domains, such as medicine, surveillance or operators fatigue monitoring.

ACKNOWLEDGEMENTS

This work was supported by the AGH University of Science and Technology under the grant no. 15/11/421.

REFERENCES

Azim, T., Jaffar, M., Ramzan, M., and Anwar, M. (2009). Automatic fatigue detection of drivers through yawning analysis. In *Signal Processing, Image Processing and Pattern Recognition*, pages 125–132, Berlin, Heidelberg. Springer Berlin Heidelberg.

Bay, H., Ess, A., Tuytelaars, T., and Van Gool, L. (2008). Speeded-up robust features (surf). *Comput. Vis. Image Underst.*, 110(3):346–359.

Csurka, G., C., R., D., L., F., J., W., and C., B. (2004). Visual categorization with bags of keypoints. workshop on statistical learning in computer vision. *International Conference on Computer Vision (ECCV 2004)*, page 1–22.

Cvetkovic, S., Schirris, J., and With, de, P. (2009). Locally-adaptive image contrast enhancement without noise and ringing artifacts. In *Proceedings of the IEEE International Conference on Image Processing (ICIP 2007), October 16-19, 2007, San Antonio, Texas*, pages 557–560, United States. Institute of Electrical and Electronics Engineers (IEEE).

Cyganek, B. (2007). *Soft System for Road Sign Detection*, pages 316–326. Springer Berlin Heidelberg, Berlin, Heidelberg.

Cyganek, B. (2013). *Object Detection and Recognition in Digital Images: Theory and Practice*. Wiley.

Cyganek, B. and Gruszczyński, S. (2014). Hybrid computer vision system for drivers' eye recognition and fatigue monitoring. *Neurocomputing*, 126:78–94.

Fan, X., Yin, B.-C., and Sun, Y.-F. (2009). Yawning detection based on gabor wavelets and lda. 35:409–413+432.

Fulkerson, B., Vedaldi, A., and Soatto, S. (2008). Localizing objects with smart dictionaries. In Forsyth, D., Torr, P., and Zisserman, A., editors, *Computer Vision – ECCV 2008*, pages 179–192, Berlin, Heidelberg. Springer Berlin Heidelberg.

Ji, Q. and Yang, X. (2002). Real-time eye, gaze, and face pose tracking for monitoring driver vigilance. 8:357–377.

Lazebnik, S., Schmid, C., and Ponce, J. (2006). Beyond bags of features: Spatial pyramid matching for recognizing natural scene categories. *2006 IEEE Computer Society Conference on Computer Vision and Pattern Recognition - Volume 2 (CVPR'06)*, page 1–22.

Lowe, D. G. (2004). Distinctive image features from scale-invariant keypoints. *Int. J. Comput. Vision*, 60(2):91–110.

Malpani, S., S, A. C., and Narasimhadhan, A. V. (2016). Thermal vision human classification and localization using bag of visual word. In *2016 IEEE Region 10 Conference (TENCON)*, pages 3135–3139.

Marzec, M., Lamża, A., Wróbel, Z., and Dziech, A. (2016). Fast eye localization from thermal images using neural networks. *Multimedia Tools and Applications*.

Miller, J. (1991). Short report: Reaction time analysis with outlier exclusion: Bias varies with sample size. *The Quarterly Journal of Experimental Psychology Section A*, 43(4):907–912.

Ribeiro, R. F., Fernandes, J. M., and Neves, A. J. R. (2017). Face detection on infrared thermal image. In *SIGNAL 2017 : The Second International Conference on Advances in Signal, Image and Video Processing*, pages 38–42. IARIA.

Saradadevi, M. and Bajaj, P. (2008). Driver fatigue detection using mouth and yawning analysis. 8.

Shah, A., Kukreja, S., Shinde, P., and Kumari, A. (2014). Yawning detection of driver drowsiness. 2.

Strąkowska, M. and Strąkowski, R. (2015). Automatic eye corners detection and tracking algorithm in sequence of thermal medical images. *Measurement Automation Monitoring*, 61(6):199–202.

Tola, E., Lepetit, V., and Fua, P. (2010). Daisy: An efficient dense descriptor applied to wide baseline stereo. *IEEE TRANS. PATTERN ANALYSIS AND MACHINE INTELLIGENCE*, 32(5).

Wang, S., Liu, Z., Shen, P., and Ji, Q. (2013). Eye localization from thermal infrared images. *Pattern Recognition*, 46(10):2613 – 2621.